BUTTERWORTH HEINEMANN

Polymer Vol. 36 No. 7, pp. 1347–1355, 1995

0032-3861/95/$10.00 + 0.00

Toughening of a trifunctional epoxy system: 1. Near infra-red spectroscopy study of homopolymer cure

R. J. Varley, G. R. Heath, D. G. Hawthorne and J. H. Hodgkin
CSIRO, Division of Chemicals and Polymers, Bayview Avenue, Clayton, Victoria 3168, Australia

and G. P. Simon*
Department of Materials Engineering, Monash University, Wellington Road, Clayton, Victoria 3168, Australia
(Received 10 May 1994)

The cure mechanism of a trifunctional epoxy resin with an amine catalyst has been studied using near infra-red spectroscopy. The concentrations of primary and secondary amine and epoxide groups have been monitored directly as a function of cure by the use of this technique. This was compared to thermal analysis of the cure process at a range of cure temperatures by d.s.c. The conversion of the various functional groups and the increase in the glass transition temperature was found to be uniquely determined by the degree of cure and unaffected by cure temperature. The primary amines were found to be largely reacted by gelation, followed by the commencement of the secondary amine reaction. By monitoring hydroxyl production it was possible to determine the degree to which side reactions (reactions other than the main epoxy/amine reaction) occurred. These side reactions, such as etherification, occurred at conversion values above gelation and become prominent at high levels of crosslinking when the reactive functionalities become strongly diffusion controlled and their movement sterically hindered. At these high conversions unreacted secondary amines become trapped in the glassy network and these groups may result in disadvantageous properties of the final material.

(Keywords: near infra-red spectroscopy; cure mechanism; trifunctional epoxy resin)

INTRODUCTION

Epoxy resins are a class of high performance thermosetting polymers widely used in the automotive, construction and aerospace industries[1]. There are also a wide range of epoxy resin systems currently being used for research purposes[2]. Most of these materials have the common feature of possessing a high crosslink density in order to achieve high modulus and strength and to exclude water from the resin matrix[3].

A high crosslink density, resulting from either low molecular weight between crosslinks or a high functionality, invariably leads to brittle polymers. A number of strategies have been employed to improve toughness and these have been recently reviewed[4,5]. The predominant method used has been the addition of a miscible rubber to the monomer mixture. This precipitates out as a fine, particulate rubbery dispersion in the solid matrix on curing and encourages a range of fracture toughening mechanisms in the solid, two-phase material. This dispersed morphology is essentially locked in by the time gelation has occurred[6]. More recently thermoplastics have been incorporated into the networks by dissolving relatively low molecular weight polymers such as poly(ether imide) and polysulfones into the epoxy monomer. The morphology required for optimum toughness in thermoplastically toughened epoxies is a co-continuous thermoplastic phase (~25 wt% thermoplastic)[7] as opposed to the need for a fine rubber dispersion such as in rubber toughening.

This paper is the first in a series of papers on cure properties, morphology and toughening of a commercial trifunctional resin used in the aerospace industry, triglycidyl *p*-amino phenol (TGAP), cured with the aromatic amine catalyst, diaminodiphenylsulfone (DDS). Despite its industrial importance[2,8], neither the TGAP homopolymer curing process nor its thermoplastic toughening capabilities have been as widely investigated as other commercial epoxy resins such as diglycidyl ether of bisphenol A (DGEBA) or tetraglycidyl-4,4-diaminodiphenylmethane (TGDDM)[9–14].

A trifunctional resin such as TGAP holds the promise of being a rigid, relatively high crosslink density material whilst still possessing some intrinsic toughness due to its lower crosslink density than the widely used commercial tetrafunctional epoxies. Some previous papers have reported toughening studies of TGAP[15–20] with varying degrees of success, depending on thermoplastic concentration, cured resin morphology, functionalization of the thermoplastic polymer phase, etc. TGAP is also a candi-

* To whom correspondence should be addressed

date for high temperature adhesive applications although it suffers from low shear strength[21]. In this series of papers we wish to draw together the results from a range of techniques which are able to monitor thermoset cure and comparatively analyse the results. These techniques include thermal analysis[22,23], dynamic mechanical spectroscopy[24,25] and dielectric spectroscopy[17,20,26,27] as they are applied to both the TGAP homopolymer and the thermoplastic blend system.

In this first paper the results of a near infra-red (n.i.r.) study of the polymerization reactions of TGAP homopolymer as a function of cure and post-cure are presented. Whilst mid i.r. spectroscopy from 1100 to 4000 cm^{-1} has been used to monitor epoxy cure[28-30] the many overlapping bands in the mid i.r. region make a clear analysis of the various chemical functionalities difficult. N.i.r. spectroscopy has been used much less to follow epoxy cure and yet amine and epoxide functionalities are clearly visible in the n.i.r. range without the same degree of band overlap as in the mid i.r. range. N.i.r. thus holds much promise as a technique for monitoring epoxy cure and has been increasingly used in recent times[31-41]. In this work we describe the utilization of n.i.r. spectroscopy in cure monitoring and correlate the results with other properties of the reacting system such as the glass transition temperature (T_g) and the degree of conversion measured by thermal techniques.

EXPERIMENTAL

Materials and sample preparation

The TGAP used was supplied by Ciba-Geigy, Australia, with the tradename of MY0510:

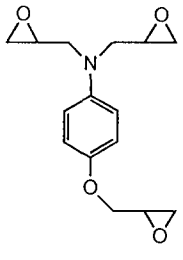

This was used without further purification and was found to have an epoxy equivalent weight of 9.41 mmol epoxy g^{-1}. The hardener, DDS, was also supplied by Ciba-Geigy and is known as HT-976 and was used as received:

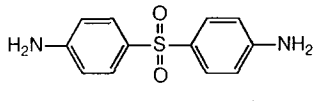

The samples were prepared by mixing the TGAP and DDS together in a ratio of 1:0.9 of epoxy to amine in a rotary evaporator in an oil bath at ~130°C until the DDS had fully dissolved in the TGAP. A slight excess of epoxy was used to simulate commercial practice where it has been found that a higher degree of conversion and a higher crosslink density can be obtained in systems with a slight epoxy excess. This relates to the kinetic difficulty of attaining full secondary amine conversion and will be examined in detail later in this paper.

Once the amine had dissolved, some 4 g of resin was poured into aluminium pans of diameter 4 cm. The resin was then cured at three temperatures (120, 140 and 160°C) and the samples were removed at appropriate time intervals so that a range of samples with different cure times could be monitored. Samples were cured isothermally for up to 10 h, after which time it was found that no further polymerization occurred. In addition, for each cure temperature, one sample was post-cured at 205°C for 2 h. As will be discussed later, the post-curing temperature was found to be sufficiently high to cause total epoxy consumption. The samples were removed from the pans and used without further preparation.

N.i.r. measurement

The transmission n.i.r. spectra of the materials were measured by an Alpha Centauri FTIR spectrophotometer (Mattson Instruments Inc., USA) which recorded spectra in the region from 9000 to 4000 cm^{-1}.

Thermal analysis

A Mettler TA4000 differential scanning calorimeter was used to assess the degree of thermal cure of samples. This was achieved by scanning a catalysed monomer sample from 50 to 300°C at various scan rates and determining the full curing exotherm by taking the average (819.5 $J g^{-1}$). Thereafter, any part-cured n.i.r. sample was scanned and the ratio of the residual exotherm to the full curing exotherm was taken as the degree of thermal cure[42]. In addition, the T_g could be determined from the d.s.c. thermogram by monitoring the endothermic changes in the thermogram. All such samples were scanned at 10°C min^{-1}.

Theory of n.i.r. analysis

The analysis described here follows that of St John and George[31] and Min *et al.*[32] although aspects of the analysis are quite different in this system because of particular overlapping peaks of the TGAP spectrum.

In order to quantify the strength of the peaks observed in the n.i.r. spectrum, Beer's Law can be used as follows:

$$A = \log(I_0/I) = \varepsilon c \ell \quad (1)$$

where A is the absorbance, I_0 is the intensity of the radiation and I is the intensity of the radiation leaving the sample. For any band ε (kg mol^{-1} cm^{-1}) is the molar absorptivity of the sample at a given wavenumber, c is the concentration of that functionality (mol kg^{-1}) and ℓ is the path length (cm) of the radiation within the sample.

In order to determine the concentration of functionalities at various stages of the cure the molar absorptivity and path length need to be known and absorbance determined experimentally. Given the difficulty in producing samples of absolute uniform thickness (and thus with a well defined path length), an internal standard peak which does not change during the cure process was used and other peaks referenced to that. Specifics of the internal peak chosen and method of calculation will be described shortly.

If an internal calibration is used, equation (1) can be written:

$$A = ac \quad (2)$$

where $a = \varepsilon \ell$ and a (kg mol^{-1}) is the effective molar absorptivity which is wavenumber dependent. Since the spectra contain some functionalities which overlap it is

necessary to assume a superposition principle, which is:

$$A = A_1 + \ldots + A_n = a_1c_1 + \ldots + a_nc_n \quad (3)$$

where A is the sum of absorbances of a combined band, $A_1 \ldots A_n$, $a_1 \ldots a_n$ and $c_1 \ldots c_n$ are the molar absorptivity and component concentrations, respectively—all at a given wavenumber. In this work, the area of the band instead of intensity was used as a measure of A_i and, for consistency, the areas were calculated over a constant wavenumber range for each band which corresponded to a particular chemical functionality.

Identification of chemical bands

The n.i.r. spectra of initial reactants TGAP and DDS are shown in *Figures 1a* and *b*, respectively. The absorption bands for the primary and secondary amine, epoxy, hydroxyl and methylene/methine groups were assigned according to the literature[36,39,43] and the values are shown in *Table 1*.

There is a large epoxy peak at 4522 cm^{-1} and weaker peaks at 5878 and 6068 cm^{-1} as seen in the monomer in *Figure 1a*. The peak at 4522 cm^{-1} is due to a combination of the epoxy C–H fundamental at 3050 cm^{-1} and the CH_2 fundamental at 1460 cm^{-1}. The peaks at 5881 and 6068 cm^{-1} are due to the first overtones of the fundamental CH_2 and CH stretches, respectively.

In the DDS spectrum (*Figure 1b*) a primary amine N–H overtone can be observed at 6627 cm^{-1} while at 5072 cm^{-1} a primary amine N–H combination peak is

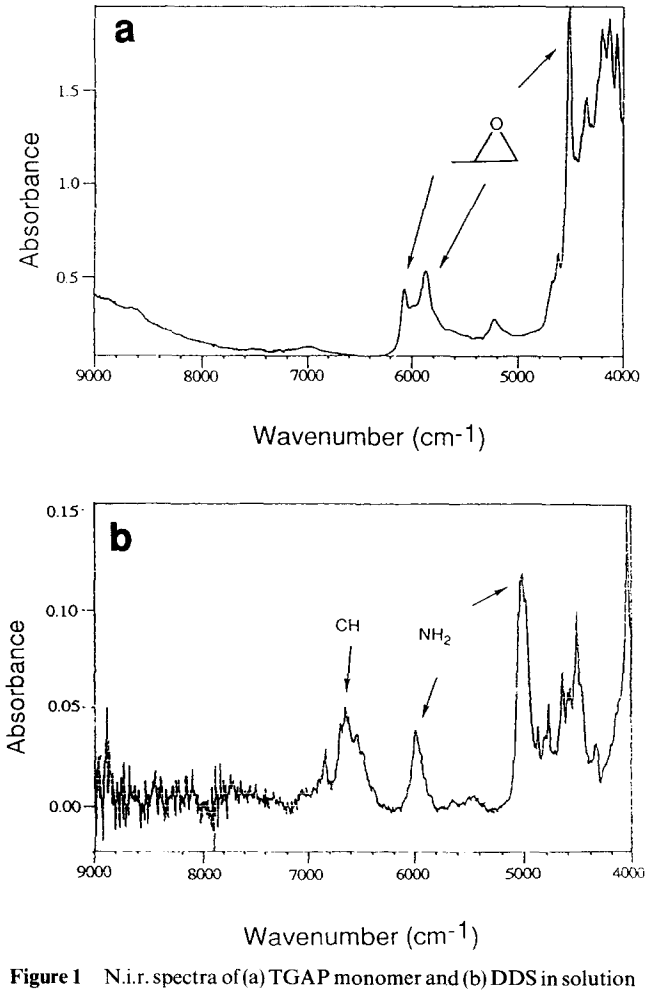

Figure 1 N.i.r. spectra of (a) TGAP monomer and (b) DDS in solution

Table 1 Band assignments for chemical groups from n.i.r. absorption spectra of TGAP/DDS

Absorption band	Observed wavenumber (cm^{-1})
Epoxide C–H	4522[a], 5881[b], 6070[b]
Primary amine N–H	4522[a], 5072[a]
Primary and secondary amine N–H	6577–6692[b]
Hydroxyl O–H	4903[a], 6990[b]
Aromatic C–H	4619[a], 4682[a], 5992[b]

[a] Combination band
[b] Overtone band

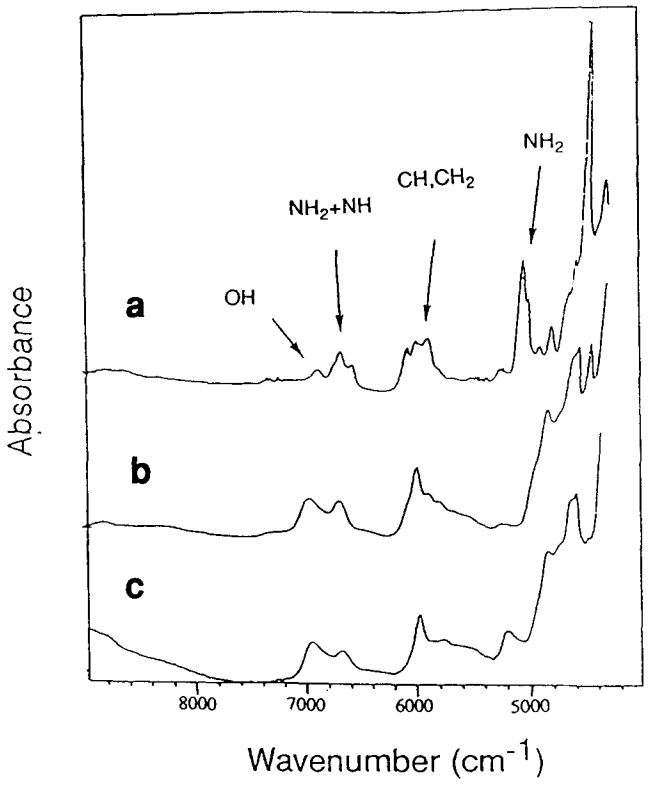

Figure 2 N.i.r. spectra of (a) an unreacted mixture of TGAP/DDS with an epoxy/amine stoichiometry of 1:0.9; (b) a TGAP/DDS mixture with an epoxy degree of conversion of $\alpha = 0.70$; (c) the post-cured TGAP/DDS system

observed. In the overtone region there is also an aromatic C–H peak at 5991 cm^{-1} present.

Figure 2a shows a typical spectrum of unreacted TGAP/DDS mixture, whilst *Figures 2b* and *c* show the spectrum after cure and post-cure, respectively. In *Figure 2a* the bands at 6577–6692 cm^{-1} are a combination of a primary and secondary amine overtone peaks whilst the peak at 4522 cm^{-1} is a combination of primary amine and epoxide peaks.

After cure and post-cure the primary amine peak at 5072 cm^{-1} has completely disappeared and the remaining peaks at 6577–6692 cm^{-1} are reduced and due to secondary amine groups only. In the same spectrum, the hydroxyl peak at 6968 cm^{-1} has grown at the expense of all three epoxy C–H peaks. The major difference between the spectra of a sample cured for a long time at an isothermal temperature and that of a post-cured sample is the complete disappearance of the C–H epoxy peaks at 4522, 6068 and 5878 cm^{-1}.

Calculation of molar absorptivities

As mentioned earlier, it was necessary in this work to use a particular peak as an internal standard between different samples and the aromatic C–H overtone peak at 5991 cm^{-1} was used. In unreacted monomer, this overlaps with the epoxy C–H overtone peaks, as seen in *Figure 3a*. The aromatic C–H peak which is used as the reference is that of the fully post-cured sample (*Figure 3b*) where the totally depleted epoxy C–H functionalities no longer contribute to the spectrum. The scaling factor is determined (using a computer program) for a sample at a given cure which allows subtraction of the aromatic C–H peak of the post-cured sample from the part-cured epoxy/aromatic C–H peak combination, leaving a well resolved epoxy C–H peak. This subtraction is demonstrated for the monomer spectra (0% conversion) shown in *Figure 3c*. This scaling factor must be determined at each conversion by this technique and then applied to all other peaks (such as amine peaks) to ensure normalization with respect to the internal standard peak. The use of such an internal calibration and subtraction technique was not required by St John and George[31] due to their use of an *in situ* n.i.r. optical fibre measurement of the same sample and may not be needed in other systems due to greater peak separation[32].

The molar absorptivity of the epoxy C–H peak at 5878 cm^{-1} can then be determined by appropriately scaling the absorbance and dividing by the initial epoxy concentration (in mol kg^{-1}) determined from stoichiometry.

The primary amine molar absorptivity at 5072 cm^{-1} in the TGAP/DDS monomer mixture can be calculated by appropriately scaling the primary amine absorbance and dividing by the stoichiometric amine concentration.

The calculation of secondary amine molar absorptivity is more involved since no secondary amine is present in the initial monomer. The secondary amine peaks are combined with those of the primary amines, in the 6577–6692 cm^{-1} region. In order to determine the secondary amine molar absorptivity, the mixture is taken to a low degree of cure where it is assumed only primary and secondary amine (but no tertiary amine) functionalities exist, i.e. no secondary amine conversion. In addition, it is assumed that there are no non-epoxy/amine reactions (such as etherification). In this work this was ~20% epoxy conversion. Since the primary amine molar absorptivity occurs in the 6577–6692 cm^{-1} region and can be determined independently in the low cured sample using the 5072 cm^{-1} region (as described above), the molar absorptivity of the secondary amine can be measured using the following equation and the appropriate scaling:

$$A_t = a_{PA}[PA]_t + a_{SA}[SA]_t \quad (4)$$

since

$$[SA]_t = [PA]_0 - [PA]_t \quad (5)$$

$$a_{SA} = \frac{A_t - a_{PA}[PA]_t}{[PA]_0 - [PA]_t} \quad (6)$$

where A_t is the total absorbance at 6577–6692 cm^{-1} at time t (~20% cure), a_{PA} and a_{SA} are the molar absorptivities of the primary and secondary amine at 6577–6692 cm^{-1}, respectively, $[PA]_0$ is the initial stoichiometric concentration of primary amine, $[PA]_t$ is the concentration of primary amine determined independently at 5072 cm^{-1} and $[SA]_t$ is the secondary amine concentration at time t.

The molar absorptivities for all functionalities were calculated for each cure temperature and are presented in *Table 2*. Henceforth, the molar absorptivity for the relevant temperature of cure was used in calculations.

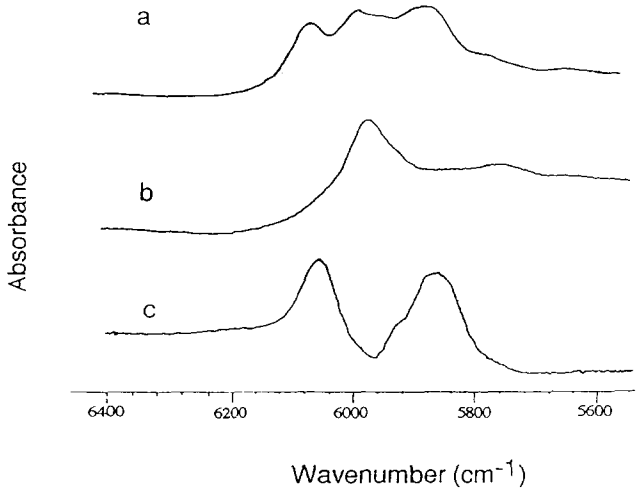

Figure 3 (a) Expanded n.i.r. spectrum of both epoxide and aromatic C–H overtone peaks of the monomer; (b) expanded spectrum of aromatic C–H peak after post-cure; (c) resultant monomer epoxy C–H overtone peak, following weighted subtraction of the aromatic C–H peak

Table 2 Molar absorptivities calculated from n.i.r. spectra for a range of cure temperatures

Molar absorptivities	Cure temperature		
	120°C	140°C	160°C
a_{epoxy} (5881 cm^{-1})	3.16	2.86	3.59
a_{PA} (5072 cm^{-1})	14.70	16.51	16.41
a_{PA} (6577–6692 cm^{-1})	8.87	8.73	10.33
a_{SA} (6577–6692 cm^{-1})	6.72	6.69	7.53

PA and SA refer to primary and secondary amine functionalities, respectively

Functional conversion analysis

Once the necessary molar absorptivities had been determined, concentrations and conversion of functionalities can be calculated in samples cured isothermally for different lengths of time.

Primary amine. Concentration of the primary amine at time t, [PA], can simply be calculated by dividing the scaled absorbance by the molar absorptivity of the primary amine at that wavelength, 5072 cm^{-1}. The degree of conversion of the primary amine, α_{PA} can be defined as:

$$\alpha_{PA} = \frac{[PA]_0 - [PA]_t}{[PA]_0} \quad (7)$$

Epoxide. The calculation of epoxide concentration was calculated similarly using the C–H epoxy peak (clearly visible following the scaled subtraction of the aromatic C–H peak from the post-cured spectrum) at 5878 cm^{-1}. The degree of epoxy conversion, α_{epoxy}, can

be determined from:

$$\alpha_{epoxy} = \frac{[EP]_t}{[EP]_0} \quad (8)$$

where $[EP]_0$ and $[EP]_t$ are the concentration of epoxide at time $t=0$ and t, respectively.

Secondary amine. The concentration of the secondary amine was calculated from the bands at 6577–6692 cm^{-1} using the equation:

$$[SA]_t = \frac{(A_t - a_{PA}[PA]_t)}{a_{SA}} \quad (9)$$

which is a combination of equations (4) and (5) and the variables are the same as described there.

The secondary amine conversion, α_{SA}, is defined as:

$$\alpha_{SA} = \frac{[PA]_0 - [PA]_t - [SA]_t}{[PA]_0} \quad (10)$$

Tertiary amine. The tertiary amine concentration is calculated by assuming that the difference between primary amine consumed and secondary amine remaining at time t is due to the formation of tertiary amine. The concentration of tertiary amine ($[TA]_t$) can thus be written:

$$[TA]_t = [PA]_0 - [PA]_t - [SA]_t \quad (11)$$

Hydroxyl. The hydroxyl concentration can be readily calculated by assuming that reactions between epoxide groups and a primary or secondary amine is the only source of hydroxyl groups. This is reasonable since side reactions such as homopolymerization or etherification do not lead to a net increase in hydroxyl concentration[31]. This indirect method of calculating hydroxyl concentration is necessary since the hydroxyl bands in the n.i.r. spectrum are split due to both free and hydrogen-bonded hydroxyl groups and thus direct calculation of concentration is difficult. The equation to calculate the hydroxyl concentration at time t, $[OH]_t$, is as follows:

$$[OH]_t = [PA]_0 - [PA]_t + [TA]_t \quad (12)$$

The degree of hydroxyl production, α_{OH}, is defined as:

$$\alpha_{OH} = \frac{[OH]_t}{[PA]_0} \quad (13)$$

All conversions described above are presented in this work as per cent conversions.

RESULTS AND DISCUSSION

The degree of conversion of the epoxide as a function of cure time was calculated both from n.i.r. and d.s.c. data for all three cure temperatures (120, 140, 160°C) and is shown in *Figure 4* for the 120°C cure. At this temperature, as for all cure temperatures, the conversions determined independently using both the n.i.r. and d.s.c. techniques were found to be almost identical. It was observed that the conversion measured from the n.i.r. was consistently a few per cent less than that measured from d.s.c. and this is reflected in the difference seen, for example, in the level of ultimate d.s.c. and n.i.r. cure. From n.i.r. the 120°C cure reaction levelled off at 69% cure while d.s.c. cure

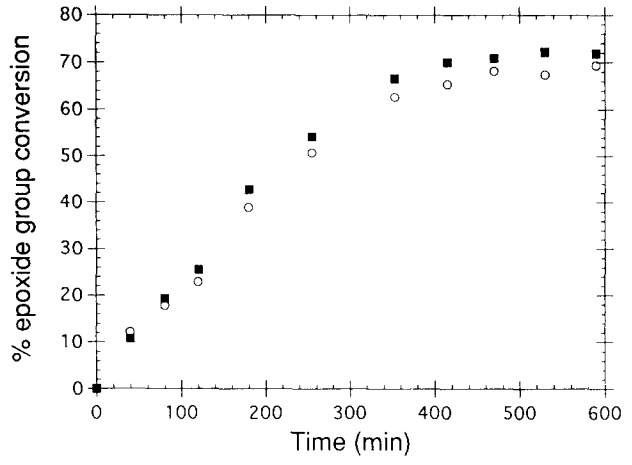

Figure 4 Comparison of epoxide conversion against cure time at 120°C determined from d.s.c. (■) and n.i.r. (○) techniques

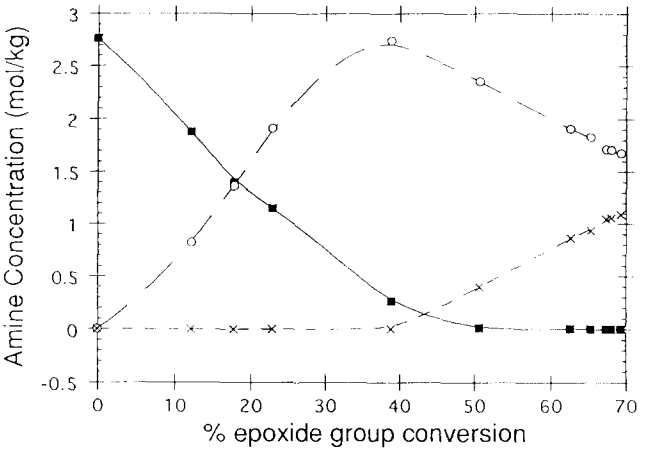

Figure 5 Primary amine (■), secondary amine (○) and tertiary amine (×) concentration as a function of per cent epoxy conversion for a cure temperature of 120°C

plateaued at 72%. Similarly for the 140°C cure cycle, ultimate n.i.r. cure was 79% whilst d.s.c. cure was 82% and for 160°C n.i.r. cure was 87% and d.s.c. cure 89% at high conversions. The similarity of the values obtained indicates the validity of the n.i.r. analysis method described earlier. The changes in concentration of the various amine functionalities were calculated using the primary amine peak and the 6577–6692 cm^{-1} peak, in conjunction with equations (7) and (8). This was determined for all three cure temperatures (120, 140 and 160°C) and as an example, *Figure 5* illustrates the change in primary, secondary and tertiary amine concentration for the 120°C cure. All the cure temperatures showed qualitatively very similar concentration *versus* time dependencies.

The primary amine concentration can be seen in *Figure 5* to decrease rapidly, as expected, at the commencement of cure. Likewise, the secondary amine concentration increases as the primary amine decreases from the commencement of cure. However, by 40% conversion the primary amines are almost totally depleted and secondary amine concentration is beginning to decrease while the production of tertiary amine becomes significant beyond 40% conversion. This is reflected for all tempera-

tures, with the higher cure temperatures exhibiting greater residual tertiary amine concentrations indicating the increased extent of network formation.

It is of interest to correlate the various changes in functional group concentration with the physical state of the resin. We have looked at such dependencies in detail and the results will be published elsewhere[44]. However, it is useful to draw upon some of those results here. The technique used to determine the physical state of the system as a function of isothermal cure time was the torsion braid method of Aronhime and Gillham[45] where two maxima are generally seen in the isothermal $\tan\delta$ *versus* cure time plot at a given cure temperature. The first peak is generally associated with gelation and the second with vitrification[45]. These results[44] indicated that in the TGAP system, gelation is relatively independent of cure temperature (varying from 38 to 42% conversion for cure temperatures ranging from 120 to 160°C). This corresponds well to the theoretical value of 41% calculated from the equation of Flory[46].

$$p_{gel}^2 = \frac{1}{(f-1)(g-1)} \tag{14}$$

where p_{gel} is the degree of conversion at which gelation occurs, and f and g are the functionalities of the TGAP epoxy monomer ($f=3$) and DDS ($g=4$). Thus, according to simple theory, gelation is dependent on the functionalities of the reacting species only, although it will be influenced by other processes such as cyclization. Vitrification, on the other hand, is dependent on the temperature of cure as illustrated by the *TTT* diagrams of Aronhime and Gillham[45]. In the TGAP system the degree of conversion at which vitrification occurs varies relatively linearly from 55% for 120°C cure to 65% for a 160°C cure cycle[44]. By reference to *Figure 5* (and corresponding data from other temperatures not shown here) it can be seen that the primary amines are essentially depleted by gelation. The maximum in secondary amine concentration which occurs near resin gelation, subsequently declines with further conversion. The concentration of tertiary amine groups at this point begins to increase, thus resulting in a rapid increase in the density of network crosslinks. By the time vitrification occurs, the concentration of secondary amine functionalities is decreasing steadily and the concentration of tertiary amines becomes significant.

It is of interest to contrast this correlation of reacted chemical groups and the physical state of the resin with other similar epoxy systems. Fortunately, other n.i.r. work that has been done with a tetrafunctional epoxy resin TGDDM[31] and the bifunctional epoxy resin DGEBA[32], has used the same catalyst, DDS, allowing elucidation of the effect of functionality. In the DGEBA system[32] it was found that, as with TGAP, the primary amines were largely converted by gelation and only beyond the gelation point did the secondary amine groups start to become significantly depleted. This was explained in terms of the polymerization of the epoxide unit reacting predominantly with the primary amine groups prior to gelation (linear polymerization)[32]. Thereafter, the reactions of secondary amines predominate and this results in significant chain branching and crosslinking. In a system in which the monomer is bifunctional, such a two-stage mechanism (sequential linear polymerization followed by crosslinking) can be readily understood. It is perhaps rather surprising in the trifunctional TGAP system that similar behaviour is also observed, since being trifunctional, reaction of the DDS primary amine with the epoxy groups will lead very rapidly to highly branched structures. St John and George[31] also found in the tetrafunctional TGDDM system that primary amines were essentially depleted by gelation. However, in the tetrafunctional system the concentration of tertiary amines was significantly higher at gelation. This means that much greater amounts of branching and crosslinking occur prior to gelation in the TGDDM system compared to lower functionality systems.

A plot of the primary and secondary amine *versus* epoxy conversion (*Figure 6*) for the three cure temperatures indicates that the data from all three isothermal cure temperatures are quite superimposable. It seems that the primary amine and secondary amine reaction mechanism is largely temperature independent and that the concentration of functional groups at any cure temperature is a function of degree of epoxide conversion.

The T_gs at various epoxy conversions were determined by d.s.c. and are also plotted for the three cure temperatures in *Figure 7*. It can be seen that the T_g increase with cure shows two regimes—a slow increase

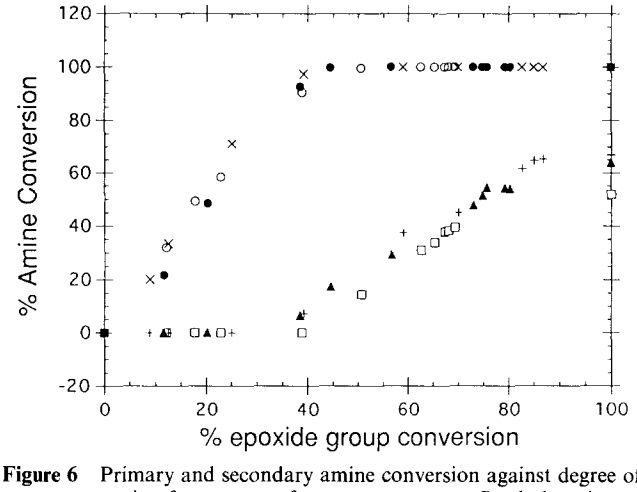

Figure 6 Primary and secondary amine conversion against degree of epoxy conversion for a range of cure temperatures. Symbols: primary amine conversion at 120°C (○), 140°C (●), 160°C (×) and secondary amine conversion at 120°C (□), 140°C (▲) and 160°C (+). The points at full epoxy conversion were obtained by post-curing the samples

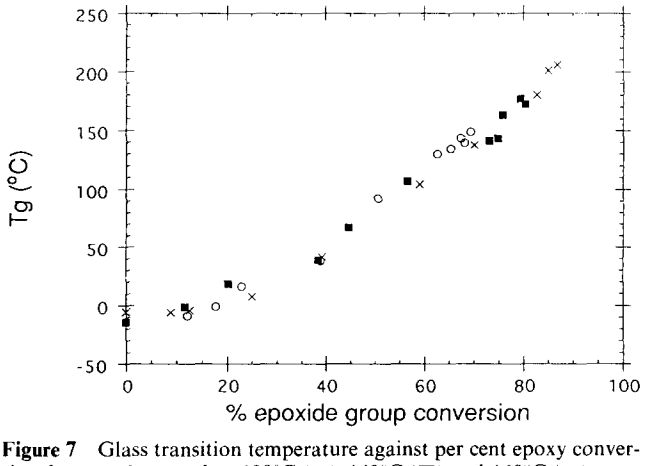

Figure 7 Glass transition temperature against per cent epoxy conversion for samples cured at 120°C (○), 140°C (■) and 160°C (×)

below the gelation region (below ~40% cure) followed by a rather more rapid increase above gelation T_g. The first increase is likely due to chain extension and production of a highly branched epoxy network prior to gelation. The rapid increase with T_g after gelation is due to the network becoming rigid because of increasing crosslinking of the highly branched regions, leading to a rapid decrease in free volume and hence an increase in T_g[47]. As with *Figure 6* where it was demonstrated that consumption of amine groups as a function of conversion was independent of temperature of cure, so too is glass transition dependent only on the degree of cure and independent of the reaction temperature that led to that degree of conversion. This has been observed and modelled recently in other epoxy systems[48].

The sequential reaction of both the amines and the two regimes of increase in glass transition is well illustrated in *Figures 8* and *9* in which the increase in T_g is plotted against consumption of primary and secondary amines, respectively. In *Figure 8*, a gradual increase in T_g is seen with primary amine conversion whereas a more rapid increase is seen during crosslinking of the highly branched polymer as indicated by the consumption of secondary amines (*Figure 9*). The T_g increase due to the primary amine epoxide chain extension reaction is

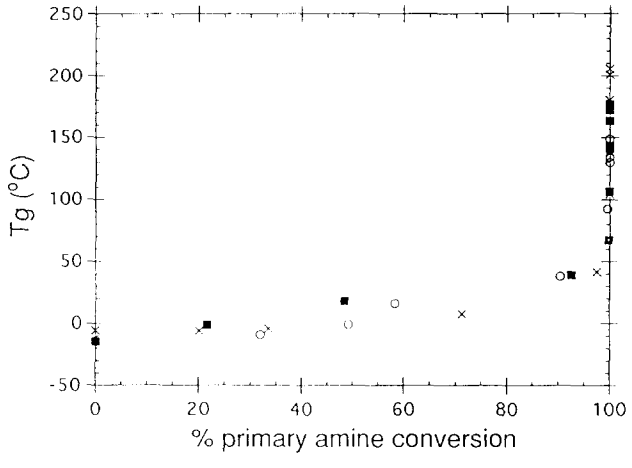

Figure 8 Glass transition temperature against per cent primary amine conversion for samples cured at 120°C (○), 140°C (■) and 160°C (×)

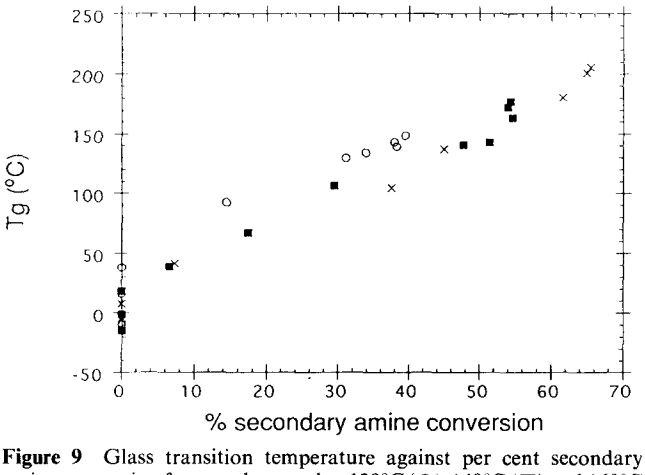

Figure 9 Glass transition temperature against per cent secondary amine conversion for samples cured at 120°C (○), 140°C (■) and 160°C (×)

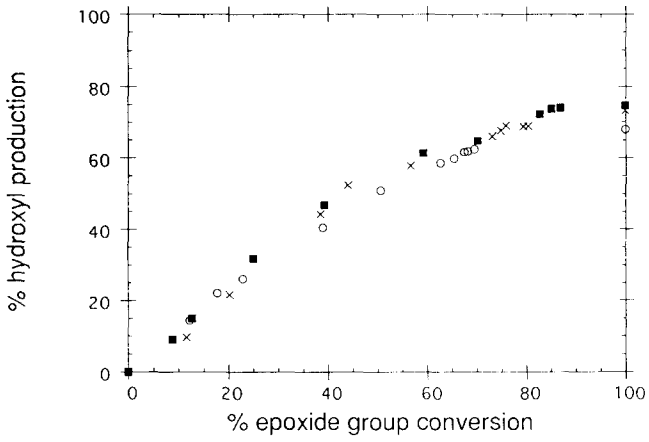

Figure 10 Per cent hydroxyl production against per cent epoxy conversion for samples cured at 120°C (○), 140°C (■) and 160°C (×). The points at full epoxy conversion were obtained by post-curing the samples

~50°C whilst the T_g increase due to secondary amine epoxide reaction is some 170°C.

The possibility of side reactions such as polyetherification and/or homopolymerization occurring have not been considered yet in this work. For a bifunctional epoxy resin system, recent work suggests that little or no side reactions occur regardless of the temperature or the conversion[32]. For a tetrafunctional system however, Chiao[49] claims that the etherification reaction only becomes important at temperatures greater than 150°C. Cole *et al.*[50] have reported that for a similar system etherification is only important at high conversions due to the catalytic effect of the tertiary amines produced while Gupta *et al.*[51] have claimed that in a tetrafunctional epoxy system etherification is the dominant reaction mechanism after vitrification. Recent work on tetrafunctional epoxy resins using n.i.r.[30,36,41] has shown that although etherification is not the dominant reaction early in the cure it is certainly not inconsequential and becomes more important at high cure conversions. A trifunctional system (such as that discussed in this work) whose functionality and gel point lie between that of the bi- and tetrafunctional epoxy systems may be expected to show behaviour somewhat intermediate in nature. A rapid rise in viscosity—as occurs near gelation—could be expected to decrease the mobility of reactive groups (particularly those attached to growing chains) and favour side reactions rather than amine–epoxide reactions.

A method of demonstrating the nature of the ongoing reaction as a function of cure is to plot n.i.r. epoxy conversion against either amine concentration or hydroxyl production. It is quite valid to plot the latter since one hydroxyl unit is produced per amine reaction (primary or secondary) and etherification is essentially hydroxyl content neutral[31] (one consumed and one formed per reaction).

If the predominant mechanism for reaction was between primary or secondary amine groups and epoxide functionalities, a straight line of slope equal to one would result for hydroxyl production *versus* epoxide conversion. Such a plot was seen in the bifunctional DGEBA/DDS system[30] and ascribed to a lack of side reactions. *Figure 10* in this paper shows the result for the TGAP/DDS system cured at the same three temperatures as before.

Rather than a simple 1:1 dependency expected for pure epoxy/amine addition, a two regime behaviour is seen with hydroxyl production exhibiting a slope of one until 40% epoxy group conversion (near gelation) and a reduced gradient until ~90% epoxy group conversion, the highest conversion attainable at the cure temperatures used. It is clear that at long cure times with all three temperatures of cure, full secondary amine and epoxy conversion is not complete. The points on the 100% epoxide conversion axis of *Figure 10* are points relating to post-cured samples (205°C for 2 h). It can be clearly seen that during post-cure there is little further hydroxyl production and that the post-curing reaction must be due to a side reaction that does not consume amine groups, such as polyetherification. Since (as shown earlier) primary amines have been depleted well before the cessation of the reaction (in fact consumed by gelation) it is clear that the remaining secondary amines are unable to react during post-cure. This indicates why (as mentioned earlier in the paper) it is not necessarily profitable to use stoichiometric amine/epoxy molar ratios. Unreacted secondary amines become trapped by spatial separation in the glassy network, even in the case of a slight epoxy excess. DeBakker *et al.*[41] showed that adding further amine (such as in a stoichiometric ratio) merely resulted in higher levels of unreacted secondary amines. It has been shown[52,53] that remnants of secondary amines trapped in the glassy network have deleterious effects on mechanical properties and increase moisture ingress.

It should be emphasized that the relationship seen in *Figure 10* prior to post-curing does not indicate anything quantitative about the relative reactivity of primary and secondary amines. The fact that primary amine conversion is almost totally complete before conversion of secondary amine commences (*Figure 6*) does lead to the conclusion that the reactivity of primary amines is greater than that of secondary amines due to the substitution effect (whereby the approach to a secondary amine is hindered by the preceding primary amine reaction). St John and George[31] have found that by using a combination of n.i.r. spectroscopy and kinetic analysis for the TGDDM/DDS system, the secondary amine is less than half as reactive as the primary amine.

We also did not attempt to distinguish in this work whether the etherification is intermolecular (crosslinking) or intramolecular (cyclization) in nature. For that matter, we have not been able to analyse the data to determine whether primary and secondary amine units are involved in cycles. This may well be important in terms of crosslink density and the resulting mechanical properties[54]. Recent work by St John[55] using n.i.r. and kinetic modelling of the cure of TGDDM indicates that significant concentrations of epoxy units are involved both in amine cyclization due to the amine/epoxide reaction and in etherification cyclization. Since the majority of etherification seems to occur at high degrees of cure in the glassy state and mostly during post-cure, such post-curing treatments are not as effective as hoped in increasing crosslink density although they are successful in 'cleaning up' epoxy groups. Although epoxy functionalities continue to react in the post-cure, this is mainly by etherification of epoxide groups, a significant proportion of which result in etherification cyclization, leaving unreacted secondary amines. It should also be noted that the temperature of cure does not have a large effect on the hydroxyl production/epoxide conversion plot. This reinforces the idea that cure temperature does not play a significant role in determining the curing mechanism.

CONCLUSIONS

In this work we have demonstrated that n.i.r. spectroscopy can supply useful quantitative data about the reaction of all major functional groups of a trifunctional epoxy/amine system.

The reaction mechanism was shown to consist largely of an initial reaction between primary amine and epoxide groups which, by gelation, largely exhausts the primary amine. This results in the generation of extended, highly branched material and a gradual increase in T_g. It is only after gelation that crosslinking starts to occur significantly, with the loss of secondary amine and a rapid increase in the T_g. It is shown that, once the sample has reached gelation, side reactions (probably etherification) are able to compete with secondary amine addition, due to the steric hindrance and spatial separation experienced by the reacting epoxide/amine units. Post-curing of this crosslinked system is shown to occur almost totally by non-amine/epoxide reactions, leaving unreacted secondary amines (even in slightly epoxy-rich formulations). This can result in cured samples with poor physical and mechanical properties. The etherification which occurs during the post-cure phase and causes the ultimate depletion of epoxy units, may be due to intramolecular cyclization reactions and may result in pendant rings and hence a lower crosslink density than intended.

REFERENCES

1 Stevens, J. R. *Adv. Mater. Processes* 1990, **35**, 137
2 Partridge, I. K. in 'Advanced Composites' (Ed. I. K. Partridge), Elsevier Applied Science, London, 1989, Ch. 1
3 Jones, F. R. in 'Chemistry and Technology of Epoxy Resin' (Ed. B. Ellis), Blackie Academic and Professional, Glasgow, 1993, Ch. 8
4 Lee, W. H. in 'Polymer Blends and Alloys' (Eds M. J. Folkes and P. S. Hope), Blackie, Cambridge, 1993, Ch. 7
5 Cantwell, W. J. and Kausch, H. H. in 'Chemistry and Technology of Epoxy Resins' (Ed. B. Ellis), Blackie, Academic and Professional, Glasgow, 1993, Ch. 5
6 Kinloch, A. J. in 'Structural Adhesives; Developments in Resins and Primers' (Ed. A. J. Kinloch), Elsevier Applied Science, London, 1986, Ch. 5
7 Carter, J. T. *Rubber Comp. Process. Applic.* 1991, **16**, 157
8 Pearce, P. J., Davidson, R. G. and Morris, C. E. M. *J. Appl. Polym. Sci.* 1982, **27**, 4501
9 McGrath, J. E., Hedrick, J. L., Yilgor, I. and Wilkes, G. L. *Polym. Bull.* 1985, **13**, 201
10 Kim, J. K. and Robertson, R. E. *J. Mater. Sci.* 1992, **27**, 161
11 Yamanoku, K. and Inoue, T. *Polymer* 1989, **30**, 662
12 Iijma, T., Sato, K., Fukuda, W. and Tomoi, T. *J. Appl. Polym. Sci.* 1993, **48**, 1859
13 Gomez, C. M. and Bucknall, C. B. *Polymer* 1993, **34**, 2111
14 Bennett, G. S., Farris, R. J. and Thompson, S. A. *Polymer* 1991, **32**, 1633
15 Bucknall, C. B. and Partridge, I. K. *Composites* 1984, **15**, 129
16 Hourston, D. J. and Lane, J. M. *Polymer* 1992, **33**, 1379
17 MacKinnon, D. J., Jenkins, S. D., McGrail, P. T. and Pethrick, R. P. *Macromolecules* 1992, **25**, 3492
18 Bucknall, C. B. and Partridge, I. K. *Polymer* 1983, **24**, 639
19 Bucknall, C. B. and Partridge, I. K. *Polym. Eng. Sci.* 1986, **26**, 54
20 MacKinnon, D. J., Jenkins, S. D., McGrail, P. T. and Pethrick, R. P. *Polymer* 1993, **34**, 3252
21 Morris, C. E. M. Personal communication, 1994

22 Cassetini, M., Salvetti, G., Tombari, E., Vevonesi, S. and Johari, G. P. *J. Appl. Polym. Sci., Polym. Phys. Edn* 1993, **31**, 199
23 Simon, S. L., Wisanrakkit, G. and Gillham, J. K. *Polym. Mater. Sci. Eng.* 1989, **61**, 799
24 Enns, J. B. and Gillham, J. K. *J. Appl. Polym. Sci.* 1983, **28**, 2567
25 Chu, H. S. and Seferis, J. C. *Polym. Comp.* 1984, **5**, 124
26 Delides, C. G., Hayward, D., Pethrick, R. and Vatalis, A. *J. Appl. Polym. Sci.* 1993, **47**, 2037
27 Mangion, M. B. M., Wang, M. and Johari, G. P. *J. Appl. Polym. Sci., Polym. Phys. Edn* 1992, **30**, 433
28 Morgan, R. J. and Mones, E. T. *J. Appl. Polym. Sci.* 1987, **33**, 999
29 Bellenger, V., Verdu, J., Francillette, J., Hoarau, P. and Morel, E. *Polymer* 1987, **28**, 1079
30 Stevens, G. C. *J. Appl. Polym. Sci.* 1981, **26**, 4259
31 St John, N. A. and George, G. A. *Polymer* 1992, **33**, 2679
32 Min, B. G., Stachurski, Z. H., Hodgkin, J. H. and Heath, G. R. *Polymer* 1993, **34**, 3620
33 Paputa Peck, M. C., Carter, R. O. and Qaderi, S. B. A. *J. Appl. Polym. Sci.* 1987, **33**, 77
34 Morgan, R. J., Kong, F.-M. and Walkup, C. M. *Polymer* 1984, **25**, 375
35 Schiering, D. A. and Katon, J. E. *J. Appl. Polym. Sci.* 1987, **34**, 2367
36 George, G. A., Cole-Clark, P., St John, N. and Friend, G. *J. Appl. Polym. Sci.* 1991, **42**, 643
37 George, G. A., Cole-Clark, P. and St John, N. *Mater. Forum* 1990, **14**, 203
38 Gallovedec, F., Costa-Torro, F., Laupretre, F. and Jasse, B. *J. Appl. Polym. Sci.* 1993, **47**, 823
39 Fu, J. H. and Schlup, J. R. *J. Appl. Polym. Sci.* 1993, **49**, 219
40 DeBakker, C. J., George, G. A., St John, N. and Fredericks, P. M. *Spectrochim. Acta* 1993, **49A**, 739
41 DeBakker, C. J., George, G. A. and St John, N. *Polymer* 1993, **34**, 716
42 Barton, J. *Adv. Polym. Sci.* 1988, **72**, 111
43 Goddu, R. F. and Delker, D. A. *Anal. Chem.* 1958, **30**, 2013
44 Varley, R. J., Hawthorne, D. G., Hodgkin, J. H. and Simon, G. P. in preparation
45 Aronhime, M. T. and Gillham, J. K. *Adv. Polym. Sci.* 1986, **78**, 83
46 Flory, P. J. 'Principles of Polymer Chemistry', Cornell University Press, Ithaca, New York, 1953
47 Horie, K., Hiura, H., Sawada, M. and Kambe, H. *J. Polym. Sci. A1* 1970, **8**, 1357
48 Wang, X. and Gillham, J. K. *J. Appl. Polym. Sci.* 1992, **45**, 2127
49 Chiao, L. *Macromolecules* 1990, **23**, 1286
50 Cole, K. C., Hechler, J. J. and Noel, D. *Macromolecules* 1991, **24**, 3098
51 Gupta, A., Cizmecioglu, M., Coulter, D., Liang, R. H., Yavrouian, H., Tsay, F. D. and Moacanin, J. J. *J. Appl. Polym. Sci.* 1983, **28**, 1011
52 Apicella, A., Nicolais, M. I. and Passerini, P. *J. Appl. Polym. Sci.* 1984, **29**, 2083
53 Apicella, A. and Nicolais, M. I. *Adv. Polym. Sci.* 1985, **72**, 69
54 Attias, J. A., Bloch, B. and Laupretre, F. *J. Polym. Sci. A* 1990, **28**, 3445
55 St John, N. *PhD thesis* University of Queensland, Australia, 1994